

A High-Order Discontinuous Galerkin Lagrange Projection Scheme for the Barotropic Euler Equations

Christophe Chalons and Maxime Stauffert

Abstract This work considers the barotropic Euler equations and proposes a high-order conservative scheme based on a Lagrange-Projection decomposition. The high-order in space and time are achieved using Discontinuous Galerkin (DG) and Runge-Kutta (RK) strategies. The use of a Lagrange-Projection decomposition enables the use of time steps that are not constrained by the sound speed thanks to an implicit treatment of the acoustic waves (Lagrange step), while the transport waves (Projection step) are treated explicitly. We compare our DG discretization with the recent one (Renac in Numer Math 1-27, 2016, [7]) and state that it satisfies important non linear stability properties. The behaviour of our scheme is illustrated by several test cases.

Keywords Barotropic Euler equations · High-order discontinuous Galerkin schemes · Lagrange-projection decomposition · Implicit explicit · Large time steps

MSC (2010): 35L40 · 35Q35 · 65M12 · 65M60

1 Introduction

We are interested in the gas dynamics equations in Eulerian coordinates

$$\begin{cases} \partial_t \rho + \partial_x(\rho u) = 0, \\ \partial_t(\rho u) + \partial_x(\rho u^2 + p) = 0, \end{cases} \quad (1)$$

C. Chalons · M. Stauffert (✉)

Laboratoire de Mathématiques de Versailles, UVSQ, CNRS,
Université Paris-Saclay, 45 avenue des États-Unis, 78035 Versailles, France
e-mail: maxime.stauffert@uvsq.fr

C. Chalons
e-mail: christophe.chalons@uvsq.fr

© Springer International Publishing AG 2017

C. Cancès and P. Omnes (eds.), *Finite Volumes for Complex Applications VIII—Hyperbolic, Elliptic and Parabolic Problems*, Springer Proceedings in Mathematics & Statistics 200, DOI 10.1007/978-3-319-57394-6_7

where $\rho > 0$ is the density, u the velocity and $p = p(\rho)$ is the pressure of the fluid such that $p'(\rho) > 0$. In the numerical experiments, we will choose $p(\rho) = g\rho^2/2$ where $g > 0$ is the gravity constant so that the model can also be understood as the Shallow-Water equations with flat topography (in this case, ρ stands for the water depth). The unknowns depend on the space and time variables x and t , with $x \in \mathbb{R}$ and $t \in [0, \infty)$. At time $t = 0$, the model is supplemented with a given initial data $\rho(x, t = 0) = \rho_0(x)$ and $u(x, t = 0) = u_0(x)$.

The aim of this paper is to propose a high-order discretization based on a Lagrange-Projection decomposition of the governing equations and using a Discontinuous Galerkin (DG) [4, 9] strategy for the space variable.

The Lagrange-Projection (or equivalently Lagrange-Remap) decomposition is interesting since it allows to naturally decouple the acoustic and transport terms of the model. It proved to be useful and very efficient when considering subsonic or low-Mach number flows. In this case, the CFL restriction of Godunov-type schemes is driven by the acoustic waves and can be very restrictive. The Lagrange-Projection strategy allows for a very natural implicit-explicit scheme with a CFL restriction based on the (slow) transport waves and not on the (fast) acoustic waves. We refer for instance the reader to [1, 2, 5], to the recent contribution [3], and to the references therein. Note that the later contribution considers the Shallow-Water equations with non flat topography and that the corresponding (implicit-explicit) Lagrange-Projection scheme is well-balanced but only first-order accurate. It is the purpose of this contribution to extend the first-order Lagrange-Projection schemes of the above references to high-order of accuracy in both space and time. The proposed approach is quite close to the one recently developed in [7], but as we will see, the corresponding Projection step turns out to be different.

2 Lagrange-Projection Decomposition and Finite-Volume Scheme

In this section, we briefly present the Lagrange-Projection decomposition considered in this paper and the corresponding first-order finite volume scheme.

Operator splitting decomposition and relaxation approximation. Using the chain rule for the space derivatives of (1), the Lagrange-Projection decomposition consists in first solving

$$\begin{cases} \partial_t \rho + \rho \partial_x u = 0, \\ \partial_t(\rho u) + \rho u \partial_x u + \partial_x p = 0, \end{cases} \quad (2)$$

which gives in Lagrangian coordinates $\tau \partial_x = \partial_m$, with $\tau = 1/\rho$,

$$\begin{cases} \partial_t \tau - \partial_m u = 0, \\ \partial_t u + \partial_m p = 0, \end{cases} \quad (3)$$

and then the transport system

$$\begin{cases} \partial_t \rho + u \partial_x \rho = 0, \\ \partial_t (\rho u) + u \partial_x (\rho u) = 0. \end{cases} \tag{4}$$

The numerical approximation of (3) and (4) will be given in the next sections but let us notice from now on that the Lagrangian system (3) will be treated considering the following relaxation approximation [6, 8],

$$\begin{cases} \partial_t \tau - \partial_m u = 0, \\ \partial_t u + \partial_m \Pi = 0, \\ \partial_t \Pi + a^2 \partial_m u = \lambda (p - \Pi). \end{cases} \tag{5}$$

Here, the new variable Π represents a linearization of the real pressure p , the constant parameter a is a linearization of the Lagrangian sound speed ρc such that the sub-characteristic condition $a > \rho c$, $c = \sqrt{p'(\rho)}$, is satisfied, and the relaxation parameter λ allows to recover $\Pi = p$ and the original system (3) in the asymptotic regime $\lambda \rightarrow \infty$. As usual, the relaxation system will be solved using a splitting strategy which consists in first setting $\Pi = p$ at initial time (which is formally equivalent to considering $\lambda \rightarrow \infty$ in (5)), and then solving the relaxation system (5) with $\lambda = 0$. *First-order numerical scheme.* The first-order finite volume scheme associated with the above decomposition and relaxation approximation is classical and given for instance in [2]. Nevertheless, it will be recovered in the DG extension proposed in the next section by setting the degree of all polynomials p to 0. Space and time will be discretized using a space step Δx and a time step Δt . We will consider a set of cells $\kappa_j = [x_{j-1/2}, x_{j+1/2})$ and instants $t^n = n \Delta t$, where $x_{j+1/2} = j \Delta x$ and $x_j = (x_{j-1/2} + x_{j+1/2})/2$ are respectively the cell interfaces and cell centers, for $j \in \mathbb{Z}$ and $n \in \mathbb{N}$.

3 Discontinuous Galerkin Discretization

We begin this section by introducing the notations of the DG discretization. Recall that the DG approach considers that the approximate solution at each time t^n is defined on each cell κ_j by a polynomial in space of order less or equal than p for a given integer $p \geq 1$ ($p = 0$ corresponds to the usual first-order and piecewise constant finite volume scheme). With this in mind, we consider the $(p + 1)$ Lagrange polynomials $\{\ell_i\}_{i=0, \dots, p}$ associated with the Gauss-Lobatto quadrature points in $[-1, 1]$. More precisely, denoting $-1 = s_0 < s_1 < \dots < s_p = 1$ the $p + 1$ Gauss-Lobatto quadrature points, ℓ_i is defined by the relations $\ell_i(s_k) = \delta_{i,k}$ for $k = 0, \dots, p$, where δ is the Kronecker symbol. Then, in each cell κ_j , we define the shifted Lagrange polynomials $\Phi_{i,j}$ by $\Phi_{i,j}(x) = \ell_i(\frac{2}{\Delta x}(x - x_j))$ and we take $\{\Phi_{i,j}\}_{i=0, \dots, p}$ as a basis for polynomials of order less or equal than p on κ_j . If we denote by $X_{\Delta x}$ the DG approximation of X , we thus have $X_{\Delta x}(x, t) = \sum_{k=0}^p X_{k,j}(t) \Phi_{k,j}(x)$, $\forall x \in \kappa_j$, where the coef-

ficients $X_{k,j}$ depend on time and correspond to the value of the numerical solution at the shifted Gauss-Lobatto quadrature points $x_{k,j} = x_j + \frac{\Delta x}{2} s_k$.

Before entering the details of the numerical approximation, let us briefly recall that the Gauss-Lobatto quadrature formula for $f : \kappa_j \times \mathbb{R}^+ \rightarrow \mathbb{R}$ writes

$$\int_{\kappa_j} f(x, t) dx \approx \frac{\Delta x}{2} \sum_{k=0}^p \omega_k f(x_{k,j}, t),$$

where ω_k are the weights of the Gauss-Lobatto quadrature. It is well-known that this formula is exact as soon as f is a polynomial of order less or equal than $(2p - 1)$ with respect to x on κ_j . Just note that the integral $\int_{\kappa_j} \Phi_{i,j}(x) \Phi_{k,j}(x) dx$ will be therefore approximated by $\frac{\Delta x}{2} \omega_i \delta_{i,k}$ in the following. At last, note that the piecewise constant case $p = 0$ can be also considered in this framework provided that we set $s_0 = 0$, $\Phi_{0,j} = 1$ and $\omega_0 = 2$.

Time discretization ($t^n \rightarrow t^{n+1}$). We begin with the acoustic step (5) with $\lambda = 0$. Multiplying the three equations by $\Phi_{i,j}$, integrating over κ_j , and considering the piecewise polynomial approximations $X_{\Delta x}$ for $X = \tau, u, \Pi$ easily leads to

$$\begin{cases} \frac{\Delta x}{2} \omega_i \partial_t \tau_{i,j}(t) - \int_{\kappa_j} \Phi_{i,j}(x) \partial_m u(x, t) dx = 0, \\ \frac{\Delta x}{2} \omega_i \partial_t u_{i,j}(t) + \int_{\kappa_j} \Phi_{i,j}(x) \partial_m \Pi(x, t) dx = 0, \\ \frac{\Delta x}{2} \omega_i \partial_t \Pi_{i,j}(t) + a^2 \int_{\kappa_j} \Phi_{i,j}(x) \partial_m u(x, t) dx = 0, \end{cases}$$

that we discretize in time by

$$\begin{cases} \tau_{i,j}^{n+1^-} = \tau_{i,j}^n + \frac{2\Delta t}{\omega_i \Delta x} \int_{\kappa_j} \Phi_{i,j}(x) \partial_m u(x, t^\alpha) dx, \\ u_{i,j}^{n+1^-} = u_{i,j}^n - \frac{2\Delta t}{\omega_i \Delta x} \int_{\kappa_j} \Phi_{i,j}(x) \partial_m \Pi(x, t^\alpha) dx, \\ \Pi_{i,j}^{n+1^-} = \Pi_{i,j}^n - a^2 \frac{2\Delta t}{\omega_i \Delta x} \int_{\kappa_j} \Phi_{i,j}(x) \partial_m u(x, t^\alpha) dx, \end{cases} \quad (6)$$

where the superscript $n + 1^-$ formally represents the fictitious time t^{n+1^-} , and $\alpha = n$ or $\alpha = n + 1^-$ if the time discretization is taken to be explicit or implicit.

As far as the transport step is concerned, the same process of reasoning leads to

$$\begin{cases} \rho_{i,j}^{n+1} = \rho_{i,j}^{n+1^-} - \frac{2\Delta t}{\omega_i \Delta x} \int_{\kappa_j} \Phi_{i,j}(x) u(x, t^\alpha) \partial_x \rho(x, t^{n+1^-}) dx, \\ (\rho u)_{i,j}^{n+1} = (\rho u)_{i,j}^{n+1^-} - \frac{2\Delta t}{\omega_i \Delta x} \int_{\kappa_j} \Phi_{i,j}(x) u(x, t^\alpha) \partial_x (\rho u)(x, t^{n+1^-}) dx. \end{cases} \quad (7)$$

Note that this transport step is always treated explicitly in time.

Volume integrals and flux calculations. Considering the acoustic step, we aim at approximating the integrals $\int_{\kappa_j} \Phi_{i,j}(x) \partial_m X(x, t^\alpha) dx$ with $X = u, \Pi$. Observe that

$$\int_{\kappa_j} \Phi_{i,j}(x) \partial_m X(x, t^\alpha) dx \approx \frac{\Delta x}{2} \omega_i \tau_{i,j}^n \partial_x X(x_{i,j}, t^\alpha) dx = \tau_{i,j}^n \int_{\kappa_j} \Phi_{i,j}(x) \partial_x X(x, t^\alpha) dx,$$

the last equality is indeed exact since X and Φ are polynomials of order less or equal than p , so that $\Phi_{i,j} \partial_x X(\cdot, t)$ is of order less or equal than $(2p - 1)$. The objective is now to use one integration by part to move the derivative from X to Φ , and to use the numerical fluxes to evaluate the interfacial terms, which gives

$$\int_{\kappa_j} \Phi_{i,j}(x) \partial_x X(x, t^\alpha) dx \approx \delta_{i,p} X_{j+1/2}^{*,\alpha} - \delta_{i,0} X_{j-1/2}^{*,\alpha} - \frac{\Delta x}{2} \sum_{k=0}^p \omega_k X_{k,j}^\alpha \partial_x \Phi_{i,j}(x_{k,j}).$$

Again, we refer the reader to [2] for the expressions of the star quantities in the above formula and the following ones, which are nothing but the numerical fluxes of the first-order finite volume scheme. At last, from (6) we obtain the acoustic step

$$\begin{cases} \tau_{i,j}^{n+1^-} = \tau_{i,j}^n + \frac{2\Delta t}{\omega_i \Delta x} \tau_{i,j}^n \left[\delta_{i,p} u_{j+1/2}^{*,\alpha} - \delta_{i,0} u_{j-1/2}^{*,\alpha} - \frac{\Delta x}{2} \sum_{k=0}^p \omega_k u_{k,j}^\alpha \partial_x \Phi_{i,j}(x_{k,j}) \right] \\ \quad = L_{i,j}^\alpha \tau_{i,j}^n, \\ u_{i,j}^{n+1^-} = u_{i,j}^n - \frac{2\Delta t}{\omega_i \Delta x} \tau_{i,j}^n \left[\delta_{i,p} \Pi_{j+1/2}^{*,\alpha} - \delta_{i,0} \Pi_{j-1/2}^{*,\alpha} - \frac{\Delta x}{2} \sum_{k=0}^p \omega_k \Pi_{k,j}^\alpha \partial_x \Phi_{i,j}(x_{k,j}) \right], \\ \Pi_{i,j}^{n+1^-} = \Pi_{i,j}^n - a^2 \frac{2\Delta t}{\omega_i \Delta x} \tau_{i,j}^n \left[\delta_{i,p} u_{j+1/2}^{*,\alpha} - \delta_{i,0} u_{j-1/2}^{*,\alpha} - \frac{\Delta x}{2} \sum_{k=0}^p \omega_k u_{k,j}^\alpha \partial_x \Phi_{i,j}(x_{k,j}) \right], \end{cases} \quad (8)$$

$$\text{with } L_{i,j}^\alpha = 1 + \frac{2\Delta t}{\omega_i \Delta x} \left[\delta_{i,p} u_{j+1/2}^{*,\alpha} - \delta_{i,0} u_{j-1/2}^{*,\alpha} - \frac{\Delta x}{2} \sum_{k=0}^p \omega_k u_{k,j}^\alpha \partial_x \Phi_{i,j}(x_{k,j}) \right].$$

Regarding the transport step, we want to evaluate the integrals

$$\int_{\kappa_j} \Phi_{i,j}(x) u(x, t^\alpha) \partial_x X(x, t^{n+1^-}) dx$$

with $X = \rho, \rho u$. The same process as before leads to

$$\begin{aligned} \int_{\kappa_j} \Phi_{i,j}(x) u(x, t^\alpha) \partial_x X(x, t^{n+1^-}) dx &= \delta_{i,p} X_{j+1/2}^{*,n+1^-} u_{j+1/2}^{*,\alpha} - \delta_{i,0} X_{j-1/2}^{*,n+1^-} u_{j-1/2}^{*,\alpha} \\ &\quad - \int_{\kappa_j} (Xu) \partial_x \Phi_{i,j} dx - X_{i,j}^{n+1^-} \int_{\kappa_j} \Phi_{i,j}(x) \partial_x u(x, t^\alpha) dx, \end{aligned}$$

where we take

$$\begin{aligned} \int_{\kappa_j} \Phi_{i,j} \partial_x u(x, t^\alpha) dx &= \delta_{i,p} u_{j+1/2}^{*,\alpha} - \delta_{i,0} u_{j-1/2}^{*,\alpha} - \frac{\Delta x}{2} \sum_{k=0}^p \omega_k u_{k,j}^\alpha \partial_x \Phi_{i,j}(x_{k,j}) \\ \text{and } \int_{\kappa_j} (Xu) \partial_x \Phi_{i,j} dx &\approx \frac{\Delta x}{2} \sum_{k=0}^p \omega_k X_{k,j}^{n+1^-} u_{k,j}^\alpha \partial_x \Phi_{i,j}(x_{k,j}). \end{aligned}$$

Conservativity property and mean values. Easy calculations not reported here show that the whole Lagrange-Projection scheme can be written as follows

$$\begin{aligned} \rho_{i,j}^{n+1} &= \rho_{i,j}^n - \frac{2\Delta t}{\omega_i \Delta x} \left[\delta_{i,p} \rho_{j+1/2}^{*,n+1-} u_{j+1/2}^{*,\alpha} - \delta_{i,0} \rho_{j-1/2}^{*,n+1-} u_{j-1/2}^{*,\alpha} - \frac{\Delta x}{2} \sum_{k=0}^p \omega_k \rho_{k,j}^{n+1-} u_{k,j}^\alpha \partial_x \Phi_{i,j}(x_{k,j}) \right], \\ (\rho u)_{i,j}^{n+1} &= (\rho u)_{i,j}^n - \frac{2\Delta t}{\omega_i \Delta x} \left[\delta_{i,p} \Pi_{j+1/2}^{*,\alpha} - \delta_{i,0} \Pi_{j-1/2}^{*,\alpha} - \frac{\Delta x}{2} \sum_{k=0}^p \omega_k \Pi_{k,j}^{n+1-} \partial_x \Phi_{i,j}(x_{k,j}) \right] \\ &\quad - \frac{2\Delta t}{\omega_i \Delta x} \left[\delta_{i,p} (\rho u)_{j+1/2}^{*,n+1-} u_{j+1/2}^{*,\alpha} - \delta_{i,0} (\rho u)_{j-1/2}^{*,n+1-} u_{j-1/2}^{*,\alpha} - \frac{\Delta x}{2} \sum_{k=0}^p \omega_k (\rho u)_{k,j}^{n+1-} u_{k,j}^\alpha \partial_x \Phi_{i,j}(x_{k,j}) \right] \end{aligned}$$

while the mean values $\bar{X}_j^{n+1} = \frac{1}{\Delta x} \int_{x_j} X(x, t^{n+1}) dx = \sum_{i=0}^p \frac{\omega_i}{2} X_{i,j}^{n+1}$ with $X = \rho, \rho u$ obey the conservative formulas

$$\begin{cases} \bar{\rho}_j^{n+1} = \bar{\rho}_j^n - \frac{\Delta t}{\Delta x} \left[\rho_{j+1/2}^{*,n+1-} u_{j+1/2}^{*,\alpha} - \rho_{j-1/2}^{*,n+1-} u_{j-1/2}^{*,\alpha} \right], \\ \overline{(\rho u)}_j^{n+1} = \overline{(\rho u)}_j^n - \frac{\Delta t}{\Delta x} \left[\Pi_{j+1/2}^{*,\alpha} + (\rho u)_{j+1/2}^{*,n+1-} u_{j+1/2}^{*,\alpha} \right. \\ \qquad \qquad \qquad \left. - \Pi_{j-1/2}^{*,\alpha} - (\rho u)_{j-1/2}^{*,n+1-} u_{j-1/2}^{*,\alpha} \right]. \end{cases} \quad (9)$$

Additional nonlinear stability properties can be proved for both the implicit and explicit schemes ($\alpha = n$ and $\alpha = n + 1^-$). In particular, we have been able to prove the positivity of the nodal densities $\rho_{i,j}^{n+1-}$ at time t^{n+1-} and of the mean densities $\bar{\rho}_j^{n+1}$ at time t^{n+1} , but also the validity of a discrete entropy inequality for the mean energy following the same lines as in [7].

Comparison with the double integration by part used in [7]. The present scheme turns out to be very close to the one recently proposed in [7], and it shares the same stability properties. However, the overall process in [7] is based on double integrations by part leading to the use of both numerical and exact fluxes at the interfaces, instead of only numerical fluxes in our approach. Interestingly, we observed that both schemes are strictly equivalent if one considers the mean values, but the nodal values turn out to be different because of the transport step. These little differences are due to the use of quadrature formulas to integrate the polynomials $Xu \partial_x \Phi_{i,j}$. In this case, the numerical integrations are not exact since polynomials $Xu \partial_x \Phi_{i,j}$ are of order $3p - 1 > 2p - 1$.

Positivity and generalized slope limiters. We have already stated the positivity of the nodal values $\rho_{i,j}^{n+1-}$ at the end of the acoustic step and of the mean values $\bar{\rho}_j^{n+1}$ at the end of the transport step. Similarly to [7], we suggest to use a positivity limiter to ensure that $\rho_{i,j}^{n+1} > 0$. More precisely, we replace $\rho_{i,j}^{n+1}$ by $\theta_j \rho_{i,j}^{n+1} + (1 - \theta_j) \bar{\rho}_j^{n+1}$, where the coefficients θ_j are taken to be $\theta_j = \min \left(1, \frac{\bar{\rho}_j^{n+1} - \varepsilon}{\bar{\rho}_j^{n+1} - \min_i \rho_{i,j}^{n+1}} \right)$. This formula ensures that if ρ is less than the threshold ε , the nodal values of the corresponding cell are corrected, using the positive mean value, towards values greater than ε . In general we set the parameter ε to $1.0e^{-10}$. Note that in the forthcoming numerical experiments, the positivity limiter is not active. In order to avoid non physical oscil-

lations, we also use the generalized slope limiters introduced in [4]. More precisely, considering the *minmod* function $m(a, b, c) = s \cdot \min(|a|, |b|, |c|)$ if

$s = \text{sign}(a) = \text{sign}(b) = \text{sign}(c)$ and 0 otherwise, the increments

$$\Delta_+ \bar{X}_j^{n+1} = \bar{X}_{j+1}^{n+1} - \bar{X}_j^{n+1}, \Delta_- \bar{X}_j^{n+1} = \bar{X}_j^{n+1} - \bar{X}_{j-1}^{n+1},$$

$$X_{j+1/2}^{-,n+1} = \bar{X}_j^{n+1} + m\left(X_{p,j}^{n+1} - \bar{X}_j^{n+1}, \Delta_+ \bar{X}_j^{n+1}, \Delta_- \bar{X}_j^{n+1}\right),$$

$$X_{j-1/2}^{+,n+1} = \bar{X}_j^{n+1} - m\left(\bar{X}_j^{n+1} - X_{0,j}^{n+1}, \Delta_+ \bar{X}_j^{n+1}, \Delta_- \bar{X}_j^{n+1}\right),$$

the new states at time t^{n+1} are defined by

$$\begin{cases} X_{i,j}^{n+1} & \text{if } X_{j+1/2}^{-,n+1} = X_{p,j}^{n+1} \text{ and } X_{j-1/2}^{+,n+1} = X_{0,j}^{n+1}, \\ \bar{X}_j^{n+1} + \frac{2}{\Delta x} (x_{i,j} - x_j) \cdot m\left(\partial_x X^{n+1}(x_j), \Delta_+ \bar{X}_j^{n+1}, \Delta_- \bar{X}_j^{n+1}\right) & \text{otherwise.} \end{cases}$$

4 Numerical Results

The aim of this section is to compare our explicit-explicit EXEX_p and implicit-explicit IMEX_p Lagrange-Projection schemes, where p refers to the polynomial order of the DG approach. The time integrations are performed using Strong Stability Preserving Runge-Kutta methods described in [4]. Recall that $p(\rho) = g\rho^2/2$ so that the parameter a is chosen locally at each interface according to $a_{j+1/2} = \kappa \max\left(\rho_j^n \sqrt{g\rho_j^n}, \rho_{j+1}^n \sqrt{g\rho_{j+1}^n}\right)$ with $\kappa = 1.01$ and $g = 9.81$. We set $\Delta t = \min(\Delta t_{\text{Lag}}, \Delta t_{\text{Tra}})$ for the EXEX_p schemes and $\Delta t = \Delta t_{\text{Tra}}$ for the IMEX_p schemes where $\Delta t_{\text{Lag}} = \frac{\Delta x}{2^{p+1}} \min_j (2a_{j+1/2} \min(\tau_{p,j}, \tau_{0,j+1}))$ is the DG time-step restriction associated with the Lagrangian step, while the Transport step CFL restriction reads $\Delta t_{\text{Tra}} = \Delta x \min_{i,j} \frac{2}{\omega_i} \left(\int_{\kappa_j} u^\alpha \partial_x \Phi_{i,j} dx - \delta_p u_{j+1/2}^{*,\alpha,-} + \delta_0 u_{j-1/2}^{*,\alpha,+} \right)$.

Manufactured smooth solution. This preliminary test case is taken from [7] and allows us to test the experimental order of accuracy (EOA) of the schemes, especially on the Transport step. The space domain is $[0, 1]$, the boundary conditions are periodic and the initial conditions are $\rho_0(x) = 1 + 0.2 \sin(2\pi x)$ and $u_0(x) = 1$. We solve (1) with a source term such that the exact solution is $\rho(x, t) = 1 + 0.2 \sin(2\pi(x - t))$ and $u(x, t) = 1$, which just means that we impose $u_{i,j}^{n+1,-} = 1$ and $\Pi_{i,j}^{n+1,-} = \Pi_{i,j}^n$, so that the Acoustic step is trivial. Note that we use in this special case the EXEX_p schemes. The EOA are reported in Table 1.

Dam break problem. In this test case, we take $\rho_0(x) = 20$ if $x \in [0, 750[$, $\rho_0(x) = 10$ if $x \in]750, 1500]$, and $u_0 = 0$ everywhere. The solutions given by the EXEX_p and IMEX_p schemes with $p = 0, 1$ and 2 are shown on Fig. 1 using a 100-cell mesh, and compared with the classical first-order HLL scheme over a 100-cell mesh and a reference 1000-cell refined mesh. Note that the slope limiters allow to reduce spurious oscillations, but there is still a little undershoot for the EXEX₁ scheme.

Table 1 EOA for the manufactured smooth solution at time $T = 0.5$

Δx	$p = 0$		$p = 1$		$p = 2$	
	$\ \rho_{\Delta x} - \rho\ _1$	order	$\ \rho_{\Delta x} - \rho\ _1$	order	$\ \rho_{\Delta x} - \rho\ _1$	order
1/512	9.3986E-03	0.9432	1.0196E-05	1.9996	1.3457E-08	2.9907
1/1024	4.7945E-03	0.9710	2.5493E-06	1.9998	1.6849E-09	2.9977
1/2048	2.4217E-03	0.9854	6.3736E-07	1.9999	2.1070E-10	2.9994

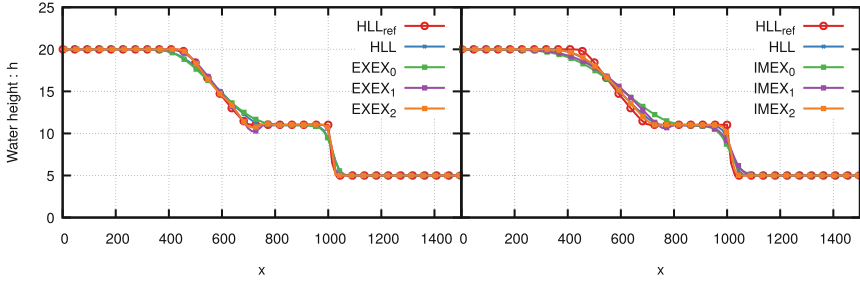


Fig. 1 Dam Break problem, water height at time $T = 10$, $EXEX_p$ (left), $IMEX_p$ (right)

Acknowledgements The authors are very grateful to P. Kestener, S. Kokh and F. Renac for stimulating discussions, and the “Maison de la Simulation” for providing excellent working conditions to the second author.

References

1. Chalons, C., Girardin, M., Kokh, S.: Large time step and asymptotic preserving numerical schemes for the gas dynamics equations with source terms. *SIAM J. Sci. Comput.* **35**(6), A2874–A2902 (2013)
2. Chalons, C., Girardin, M., Kokh, S.: An all-regime Lagrange-Projection like scheme for the gas dynamics equations on unstructured meshes. *Commun. Comput. Phys.* **20**(01), 188–233 (2016)
3. Chalons, C., Kestener, P., Kokh, S., Stauffert, M.: A large time-step and well-balanced Lagrange-Projection type scheme for the shallow-water equations. *Communic. Math. Sci.* **15**(3), 765–788 (2017)
4. Cockburn, B., Shu, C.W.: Runge-Kutta discontinuous Galerkin methods for convection-dominated problems. *J. Sci. Comput.* **16**(3), 173–261 (2001)
5. Coquel, F., Nguyen, Q., Postel, M., Tran, Q.: Entropy-satisfying relaxation method with large time-steps for Euler IBVPs. *Math. Comput.* **79**, 1493–1533 (2010)
6. Jin, S., Xin, Z.P.: The relaxation schemes for systems of conservation laws in arbitrary space dimension. *Comm. Pure Appl. Math.* **48**(3), 235–276 (1995)
7. Renac, F.: A robust high-order Lagrange-Projection like scheme with large time steps for the isentropic Euler equations. *Numer. Math.*, 1–27 (2016)
8. Suliciu, I.: On the thermodynamics of fluids with relaxation and phase transitions. *Fluids with relaxation. Internat. J. Engrg. Sci.* **36**, 921–947 (1998)
9. Xing, Y., Zhang, X., Shu, C.W.: Positivity-preserving high order well-balanced discontinuous Galerkin methods for the shallow water equations. *Adv. Water Resour.* **33**(12), 1476–1493 (2010)